ELSEVIER

Journal of Fluids and Structures 21 (2005) 579–595

JOURNAL OF FLUIDS AND STRUCTURES

www.elsevier.com/locate/jfs

Nonlinear vibrations of fluid-filled clamped circular cylindrical shells

K.N. Karagiozis[a], M. Amabili[b], M.P. Païdoussis[a,*], A.K. Misra[a]

[a]*Department of Mechanical Engineering, McGill University, 817 Sherbrooke Street West, Montreal, Québec, Canada H3A 2K6*
[b]*Dipartimento di Ingegneria Industriale, Università di Parma, Parco Area delle Scienze 181/A, Parma I-43100, Italy*

Received 1 April 2005; accepted 27 July 2005
Available online 28 October 2005

Abstract

In this study, the nonlinear vibrations are investigated of circular cylindrical shells, empty or fluid-filled, clamped at both ends and subjected to a radial harmonic force excitation. Two different theoretical models are developed. In the first model, the standard form of the Donnell's nonlinear shallow-shell equations is used; in the second, the equations of motion are derived by a variational approach which permits the inclusion of constraining springs at the shell extremities and taking in-plane inertial terms into account. In both cases, the solution includes both *driven* and *companion* modes, thus allowing for a travelling wave in the circumferential direction; they also include axisymmetric modes to capture the nonlinear inward shell contraction and the correct type (softening) nonlinear behaviour observed in experiments. In the first model, the clamped beam eigenfunctions are used to describe the axial variations of the shell deformation, automatically satisfying the boundary conditions, leading to a 7 degree-of-freedom (dof) expansion for the solution. In the second model, rotational springs are used at the ends of the shell, which when large enough reproduce a clamped end; the solution involves a sine series for axial variations of the shell deformation, leading to a 54 dof expansion for the solution. In both cases the modal expansions satisfy the boundary conditions and the circumferential continuity condition exactly. The Galerkin method is used to discretize the equations of motion, and AUTO to integrate the discretized equations numerically. When the shells are fluid-filled, the fluid is assumed to be incompressible and inviscid, and the fluid–structure interaction is described by linear potential flow theory. The results from the two theoretical models are compared with existing experimental data, and in all cases good qualitative and quantitative agreement is observed.

Keywords: Shell vibrations; Nonlinear dynamics; Donnell equations; Analytical models; Clamped ends; Comparison to experiments

1. Introduction

An extensive review on geometrically nonlinear (large-amplitude) shell vibrations has recently been provided by Amabili and Païdoussis (2003); see also Païdoussis (2003). From this review emerges the fact that most of the literature deals with simply supported shells. Not many studies on shells with other boundary conditions are available; some of the most important ones will be discussed in the following.

*Corresponding author.
E-mail address: mary.fiorilli@mcgill.ca (M.P. Païdoussis).

0889-9746/$ - see front matter © 2005 Elsevier Ltd. All rights reserved.
doi:10.1016/j.jfluidstructs.2005.07.020

Nomenclature

E	Young's modulus
$\tilde{f},\bar{f}$	force excitation
h	shell thickness
k	stiffness of the rotational distributed springs at the ends of the shell
k_x, k_θ, $k_{x\theta}$	changes in curvature and torsion
L	shell length
m	number of axial half-waves
n	number of circumferential waves
N_x, N_y, N_{xy}	stress resultants per unit length
R	shell radius
t	time
$u(x,\theta,t)$	axial shell displacement
$u_{m,n,c}(t)$, $u_{m,n,s}(t)$	modal coordinates of axial displacement (time dependent)
$v(x,\theta,t)$	circumferential shell displacement
$v_{m,n,c}(t)$, $v_{m,n,s}(t)$	modal coordinates of circumferential displacement (time dependent)
$w(x,\theta,t)$	radial shell displacement
$w_{m,n,c}(t)$, $w_{m,n,s}(t)$	modal coordinates of radial displacement (time dependent)
x, y, z	longitudinal, circumferential, radial coordinates
ε_x, ε_θ, $\gamma_{x\theta}$	shell strains
$\varepsilon_{x,0}$, $\varepsilon_{\theta,0}$, $\gamma_{x\theta,0}$	middle surface strains
$\zeta_{1,n}$	modal damping coefficient of mode $(1,n)$
θ	angular coordinate
λ_m	dimensionless mth mode eigenvalue of a clamped–clamped beam (Model 1)
λ_m	$m\pi/L$ in Model 2
ρ_S	mass density of the shell
φ_m	dimensionless beam eigenfunction associated with eigenvalue λ_m
Φ	velocity potential of the fluid
ω	force excitation frequency
$\omega_{1,n}$	fundamental frequency of first longitudinal and nth circumferential mode

Matsuzaki and Kobayashi (1969) studied theoretically and experimentally large-amplitude vibrations of clamped circular cylindrical shells. They based their analysis on Donnell's nonlinear shallow-shell theory and used a simple mode expansion with 2 degrees of freedom (dof). The analysis predicted a softening type nonlinearity for clamped shells, in agreement with their own experimental results. They also found amplitude-modulated response close to resonance and identified it as a beating phenomenon due to frequencies very close to the excitation frequency.

Chia (1987a, b) studied nonlinear free vibrations and postbuckling of symmetrically and asymmetrically laminated circular cylindrical panels with imperfections and different boundary conditions. Donnell's nonlinear shallow-shell theory was used. A single-mode analysis was carried out, and the results showed a hardening nonlinearity. Iu and Chia (1988) used Donnell's nonlinear shallow-shell theory to study free vibrations and post-buckling of clamped and simply supported, asymmetrically laminated cross-ply circular cylindrical shells. A multi-mode expansion was used without considering the companion mode. Radial geometric imperfections were taken into account. The homogeneous solution of the stress function was retained, but the dependence on the axial coordinate was neglected. The discretized equations of motion were obtained by using the Galerkin method and were studied by harmonic balance. Three asymmetric and three axisymmetric modes were used in the numerical calculations. In a later paper, Fu and Chia (1993) included in their model nonuniform boundary conditions around the edges. Softening or hardening type nonlinearity was found, depending on the radius-to-thickness ratio. Only undamped free vibrations and buckling were investigated in all this series of studies.

Large-amplitude vibrations of two vertical clamped circular cylindrical shells, partially filled with water to different levels were studied experimentally by Chiba (1993). In this case, the responses displayed a general softening nonlinearity. The shells tested showed a larger nonlinearity when partially filled, as compared to the empty and completely filled cases. The softening type of nonlinearity was also observed in the large-amplitude vibrations of four axially loaded, clamped circular cylindrical shells made of aluminum, studied experimentally by Gunawan (1998).

Amabili (2003a) investigated large-amplitude vibrations of circular cylindrical shells with different boundary conditions and subjected to radial harmonic excitation in the spectral neighbourhood of the lowest resonances. In particular, simply supported shells with either allowed or constrained axial displacements at the edges were studied; in both cases the radial and circumferential displacements at the shell edges were constrained. Elastic rotational constraints were assumed; they allow simulating any condition from simply supported to perfectly clamped, by varying the stiffness of this elastic constraint. Two different nonlinear, thin shell theories, namely Donnell's and Novozhilov's, were used to calculate the elastic strain energy. Geometric imperfections were taken into account.

In contrast, the literature on large-amplitude vibrations of simply supported shells with and without fluid–structure interaction is much richer; e.g., see Dowell and Ventres (1968), Gonçalves and Batista (1988), Kobayashi and Leissa (1995), Amabili et al. (1999, 2000, 2003b,c), and the references cited therein.

In this paper, two theoretical models are formulated for the nonlinear dynamics of thin cylindrical shells with clamped ends, either empty or filled with dense fluid.

Model 1 utilizes the classical form of the Donnell's nonlinear shallow-shell equations, involving two coupled nonlinear equations in the radial displacement and an Airy stress function. These equations, being available, for instance in Donnell (1976) and Yamaki (1984), are not derived here ab initio. In this case the formulation applies exclusively to shells with clamped ends, and the clamped-beam eigenfunctions are used to describe the axial variation of the radial deformation. The discretized equations are obtained by means of the Galerkin method, yielding a 7 dof model.

Model 2, which is the more sophisticated model, uses the Hamiltonian (variational) framework, leading to a Lagrangian derivation of the discretized equations of motion (after appropriate modal expansions are used to accomplish this discretization). It is based on the full form of the Donnell's nonlinear shell theory, and thus involves three equations, and all three of the longitudinal (u), circumferential (v) and radial (w) displacements of the middle surface of the shell. The formulation is sufficiently general to be used for shells with supports ranging from simple supports to clamped ones. Thus, so far as the axial component of the shell deformation is concerned, a Fourier sine series is employed. The final discretized model is one of 54 dof.

In both cases, fundamentally the same linear fluid–structure interaction model is used—linear because nonlinearities associated with shell movements of the order of the shell thickness are negligible for the fluid, even though they are not for the shell itself.

2. Theoretical considerations

Two different models have been used in the present analysis. Model 1 has been specifically developed in the present study to deal with shells with clamped extremities. It involves a reduced number of dof. Model 2 has been developed by Amabili (2003a) and has been used here as a reference. It is very flexible as far as boundary conditions are concerned but involves a significant number of dof. The derivation of the equation of motion for each model is given in some detail in the following paragraphs.

Fig. 1 shows the system under consideration. It consists of a thin circular cylindrical shell of length L, mean radius R, and thickness h, such that $h/R \ll 1$. The shell ends are assumed to be clamped. The origin of the cylindrical coordinate system, $(O; x, y, z)$, is positioned at the centre of one end of the shell. The shell is assumed to be of homogeneous, isotropic elastic material of Young's modulus E and Poisson's ratio ν.

2.1. Formulation of Model 1

Model 1 is based on Donnell's nonlinear shallow-shell theory, which has the following limitations: (a) it is accurate for higher circumferential wavenumbers n ($1/n^2 \ll 1$, i.e., the minimum number of nodal diameters should be $n = 4$ or 5); (b) the in-plane inertia, transverse shear deformation and rotary inertia are neglected, making the theory valid for very thin shells, i.e., $h \ll R$, to capture moderate radial amplitudes of the order of the shell thickness (assuming that $|u|, |v| \ll h$); (c) secondary nonlinear effects such as the nonlinearities in curvature strains are neglected.

Assuming a positive radial deformation w inwards, as in Fig. 1(a), the simplified version of Donnell's nonlinear shallow-shell equation is given by

$$D\nabla^4 w + ch\dot{w} + \rho_S h\ddot{w} = f - p + \frac{1}{R}\frac{\partial^2 F}{\partial x^2} + \left(\frac{\partial^2 F}{\partial y^2}\frac{\partial^2 w}{\partial x^2} - 2\frac{\partial^2 F}{\partial x \partial y}\frac{\partial^2 w}{\partial x \partial y} + \frac{\partial^2 F}{\partial x^2}\frac{\partial^2 w}{\partial y^2}\right), \tag{1}$$

where F is the in-plane Airy stress function which satisfies the following compatibility equation:

$$\frac{1}{Eh}\nabla^4 F = -\frac{1}{R}\frac{\partial^2 w}{\partial x^2} - \frac{\partial^2 w}{\partial x^2}\frac{\partial^2 w}{\partial y^2} + \left(\frac{\partial^2 w}{\partial x \partial y}\right)^2, \tag{2}$$

where $D = Eh^3/[12(1-\nu^2)]$ is the flexural stiffness of the shell, c the structural damping coefficient, f represents the summation of all the external forces acting on the surface per unit area of the shell in the radial direction, and p the transmural pressure acting on the surface of the shell. The biharmonic operator is defined as $\nabla^4 = [\partial^2(\,)/\partial x^2 + \partial^2(\,)/\partial y^2]^2$, and the overdot denotes a time derivative.

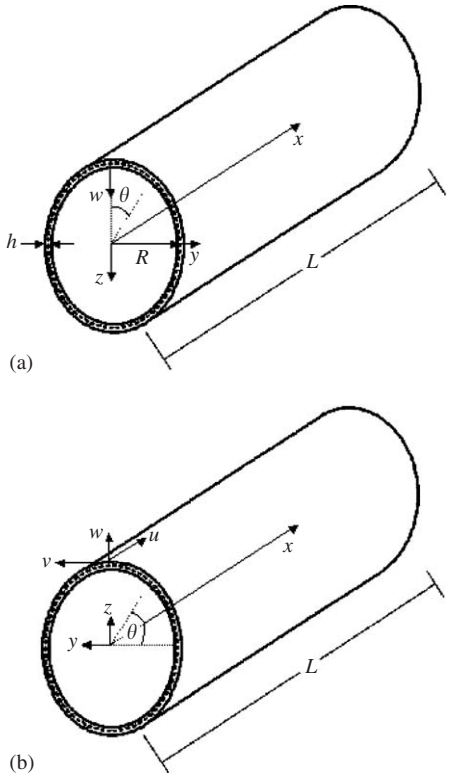

Fig. 1. Shell geometry and origin of coordinate system: (a) for Model 1; (b) for Model 2.

The expressions for the stress resultants per unit length in the axial and circumferential directions along with the shear stress resultant are given by

$$N_x = \frac{\partial^2 F}{\partial y^2}, \quad N_y = \frac{\partial^2 F}{\partial y^2}, \quad N_{xy} = -\frac{\partial^2 F}{\partial x \partial y}. \tag{3}$$

The strain–displacement relations are given by

$$\begin{aligned}
(1-\nu^2)\frac{N_x}{Eh} &= -\frac{\nu w}{R} + \frac{1}{2}\left(\frac{\partial w}{\partial x}\right)^2 + \frac{\nu}{2}\left(\frac{\partial w}{\partial y}\right)^2 + \frac{\partial u}{\partial x} + \nu\frac{\partial v}{\partial y},\\
(1-\nu^2)\frac{N_y}{Eh} &= -\frac{w}{R} + \frac{\nu}{2}\left(\frac{\partial w}{\partial x}\right)^2 + \frac{1}{2}\left(\frac{\partial w}{\partial y}\right)^2 + \nu\frac{\partial u}{\partial x} + \frac{\partial v}{\partial y},\\
(1-\nu^2)\frac{N_{xy}}{Eh} &= 2(1-\nu)\left[\frac{\partial w}{\partial x}\frac{\partial w}{\partial y} + \frac{\partial u}{\partial y} + \frac{\partial v}{\partial x}\right].
\end{aligned} \tag{4}$$

2.2. Formulation of Model 2

In contrast to Model 1, the fuller form of Donnell's shallow-shell theory is used here, involving three equations of motion. Moreover, a variational approach derivation allows the easy inclusion of constraining springs at the shell extremities. Along the middle surface of the shell the displacement components are denoted by u, v, and w, in the axial, circumferential and radial direction, respectively. Fig. 1(b) shows the same system considered in Section 2.1, but with a different convention for the axes and the shell displacements; notably, w in this case is positive outwards.

The strain components ε_x, ε_θ and $\gamma_{x\theta}$ at an arbitrary point of the shell are related to the middle surface strains $\varepsilon_{x,0}$, $\varepsilon_{\theta,0}$ and $\gamma_{x\theta,0}$ and to the changes in the curvature and torsion of the middle surface k_x, k_θ and $k_{x\theta}$ by the following

relationships (Leissa, 1973; Yamaki, 1984):

$$\varepsilon_x = \varepsilon_{x,0} + zk_x, \quad \varepsilon_\theta = \varepsilon_{\theta,0} + zk_\theta, \quad \gamma_{x\theta} = \gamma_{x\theta,0} + zk_{x\theta}, \tag{5}$$

where z is the distance of the arbitrary point of the shell from the middle surface.

According to Donnell's nonlinear shell theory, the middle surface strain–displacement relationships and changes in the curvature and torsion for a circular cylindrical shell (Yamaki, 1984) are given by

$$\varepsilon_{x,0} = \frac{\partial u}{\partial x} + \frac{1}{2}\left(\frac{\partial w}{\partial x}\right)^2, \tag{6a}$$

$$\varepsilon_{\theta,0} = \frac{1}{R}\frac{\partial v}{\partial \theta} + \frac{w}{R} + \frac{1}{2R^2}\left(\frac{\partial w}{\partial \theta}\right)^2, \tag{6b}$$

$$\gamma_{x\theta,0} = \frac{1}{R}\frac{\partial u}{\partial \theta} + \frac{\partial v}{\partial x} + \frac{1}{R}\frac{\partial w}{\partial \theta}\frac{\partial w}{\partial x}, \tag{6c}$$

$$k_x = -\frac{\partial^2 w}{\partial x^2}, \tag{6d}$$

$$k_\theta = -\frac{1}{R^2}\frac{\partial^2 w}{\partial \theta^2}, \tag{6e}$$

$$k_{x\theta} = -\frac{2}{R}\frac{\partial^2 w}{\partial x \partial \theta}. \tag{6f}$$

The elastic strain energy U_S of a circular cylindrical shell, neglecting stress σ_z according to Love's first approximation assumptions, is given (Leissa, 1973) by

$$U_S = \frac{1}{2}\int_0^{2\pi}\int_0^L\int_{-h/2}^{h/2}(\sigma_x\varepsilon_x + \sigma_\theta\varepsilon_\theta + \tau_{x\theta}\gamma_{x\theta})\,\mathrm{d}x R(1 + z/R)\,\mathrm{d}\theta\,\mathrm{d}z; \tag{7}$$

the stresses σ_x, σ_θ and $\tau_{x\theta}$ are related to the strain for homogeneous and isotropic materials, with $\sigma_z = 0$ in the case of plane stress (Leissa, 1973) by

$$\sigma_x = \frac{E}{1-\nu^2}(\varepsilon_x + \nu\varepsilon_\theta),\ \sigma_\theta = \frac{E}{1-\nu^2}(\varepsilon_\theta + \nu\varepsilon_x),\ \tau_{x\theta} = \frac{E}{2(1+\nu)}\gamma_{x\theta}. \tag{8}$$

By using Eqs. (5), (7) and (8), the following expression is obtained:

$$\begin{aligned} U_S = {} & \frac{1}{2}\frac{Eh}{1-\nu^2}\int_0^{2\pi}\int_0^L\left(\varepsilon_{x,0}^2 + \varepsilon_{\theta,0}^2 + 2\nu\varepsilon_{x,0}\varepsilon_{\theta,0} + \frac{1-\nu}{2}\gamma_{x\theta,0}^2\right)\mathrm{d}x\,R\,\mathrm{d}\theta \\ & + \frac{1}{2}\frac{Eh^3}{12(1-\nu^2)}\int_0^{2\pi}\int_0^L\left(k_x^2 + k_\theta^2 + 2\nu k_x k_\theta + \frac{1-\nu}{2}k_{x\theta}^2\right)\mathrm{d}x\,R\,\mathrm{d}\theta. \end{aligned} \tag{9}$$

The first term in Eq. (9) is the membrane (also referred to as stretching) energy, and the second one is the bending energy.

Neglecting rotary inertia, the kinetic energy T_S of a circular cylindrical shell is given by

$$T_S = \frac{1}{2}\rho_S h\int_0^{2\pi}\int_0^L(\dot{u}^2 + \dot{v}^2 + \dot{w}^2)\,\mathrm{d}x R\,\mathrm{d}\theta, \tag{10}$$

where ρ_s is the mass density of the shell; the overdot denotes a time derivative.

The final equations of motion are derived from the expressions of U_S and T_S by means of variational techniques.

2.3. Boundary conditions

The boundary conditions for Model 1 are

$$u = v = w = 0 \text{ and } \partial w/\partial x = 0 \text{ at } x = 0 \text{ and } x = L. \tag{11}$$

Since the clamped–clamped beam eigenfunctions are used to describe the axial variations in $w(x, \theta, t)$, all these boundary conditions are automatically satisfied.

The boundary conditions for Model 2 are given by

$$u = v = w = 0, \text{ at } x = 0, L, \tag{12a–c}$$

$$M_x = -k(\partial w/\partial x), \text{ at } x = 0, L, \tag{12d}$$

where M_x is the bending moment per unit length and k the stiffness per unit length of the elastic, distributed rotational springs placed at $x = 0$, L. The boundary conditions (12a)–(12c) restrain all the shell displacements at both edges. Eq. (12d) represents the case of an elastic rotational constraint at the shell edges. For a simple support, $k \to 0$ ($M_x = 0$, unconstrained rotation), while a clamped end can be achieved by taking $k \to \infty$ (zero rotation, $\partial w/\partial x = 0$); this approach is usually referred to as the artificial spring method (Yuan and Dickinson, 1992), which can be regarded as a variant of the classical penalty method. The values of the spring stiffness simulating a clamped shell can be obtained by trial and error or by evaluating the edge stiffness of the shell. In fact, it was found (Amabili and Garziera, 2000) that the natural frequencies of the system converge asymptotically to those of a clamped shell when k becomes very large.

In addition to the essential boundary conditions, both models must satisfy the condition of the circumferential continuity of the shell and be continuous in u and w.

2.4. Modal expansion

In order to reduce the continuous system to one of finite dimension, i.e., to discretize the system, the middle surface displacements u, v and w (only w in Model 1), are expanded by using approximation functions, i.e., using an appropriate set of basis functions. It is necessary to consider, in addition to the asymmetric mode directly driven into vibration by the excitation (driven mode), (i) the orthogonal mode having the same shape and natural frequency but rotated by $\pi/(2n)$ (companion mode), (ii) additional asymmetric (both driven and companion) modes, and (iii) axisymmetric modes. It has firmly been established that, for large-amplitude shell vibrations, the deformation of the shell involves significant axisymmetric oscillations inwards.

2.4.1. Modal expansion for Model 1

The modal expansion for w in Model 1 is taken as

$$w = \sum_{m=1}^{M}\sum_{n=1}^{N}(A_{m,n}(t)\cos(ny/R) + B_{m,n}(t)\sin(ny/R))\varphi_m + \sum_{m=1}^{M} A_{2m-1,0}(t)\varphi_{2m-1}, \tag{13}$$

where φ_m are the dimensionless eigenfunctions for a clamped–clamped beam defined by

$$\varphi_m = \cosh(\lambda_m x/L) - \cos(\lambda_m x/L) - \frac{\cosh(\lambda_m) - \cos(\lambda_m)}{\sinh(\lambda_m) - \sin(\lambda_m)}(\sinh(\lambda_m x/L) - \sin(\lambda_m x/L)), \tag{14}$$

λ_m being the corresponding dimensionless eigenvalues; m the axial wavenumber (equal to the number of half-waves along the shell), and n the circumferential wavenumber. The amplitude functions, $A_{m,n}(t)$, $B_{m,n}(t)$ and $A_{2m-1,0}(t)$, are the unknown generalized time functions of the vibration.

The first term of the expansion in Eq. (13), i.e., the double summation, involves the interaction between the linear asymmetric circumferential modes of nodal diameter $n > 0$, and all of the corresponding linear axisymmetric-longitudinal modes of m half-waves; this term consists of the *driven mode* along with its *companion mode*. The second term of the expansion involves all the axisymmetric-longitudinal modes, with $n = 0$. This second term has been shown to be very important in the stability analysis of the shell (Amabili et al., 1999) for simply supported shells. In the second term of the expansion, even axisymmetric modes are neglected, because these modes do not contribute to the shell contraction (the even m contractions along the length of the shell cancel out, having a zero average radial deformation).

The modal expansion given in Eq. (13) satisfies exactly the boundary conditions given in Eq. (11). The solution also satisfies exactly both the circumferential continuity and axial displacement conditions below:

$$\int_0^{2\pi R} \frac{\partial v}{\partial y}\,\mathrm{d}y = 0, \tag{15}$$

$$\int_0^{2\pi R}\int_0^{L} \frac{\partial u}{\partial x}\,\mathrm{d}x\,\mathrm{d}y = 0. \tag{16}$$

An important advantage of the expansion in Eq. (13) is the orthogonality property of the eigenfunctions involved in the summation, which simplifies the derivation of the equations of motion for the shell system.

In the present analysis the modal solution, w, given in Eq. (13), is expanded into a 7 dof model, as shown below:

$$w(x,y,t) = \left(A_{1,n}(t)\cos\left[\frac{ny}{R}\right] + B_{1,n}(t)\sin\left[\frac{ny}{R}\right]\right)\varphi_1(x) + \left(A_{2,n}(t)\cos\left[\frac{ny}{R}\right] + B_{2,n}(t)\sin\left[\frac{ny}{R}\right]\right)\varphi_2(x) + A_{1,0}(t)\varphi_1(x) + A_{3,0}(t)\varphi_3(x) + A_{5,0}(t)\varphi_5(x). \tag{17}$$

The convergence of Model 1 with 7 dof will be tested by comparison to the results of Model 2, those of a finite element code, and to experimental data available in the literature.

2.4.2. Modal expansion for Model 2

In Model 2, the displacements u, v and w can be expanded by using the following expressions, which satisfy identically boundary conditions (12a–c):

$$u(x,\theta,t) = \sum_{m=1}^{M_1}\sum_{j=1}^{N}\left[u_{m,j,c}(t)\cos(j\theta) + u_{m,j,s}(t)\sin(j\theta)\right]\sin(\lambda_m x) + \sum_{m=1}^{M_2} u_{m,0}(t)\sin(\lambda_m x), \tag{18a}$$

$$v(x,\theta,t) = \sum_{m=1}^{M_1}\sum_{j=1}^{N}\left[v_{m,j,c}(t)\sin(j\theta) + v_{m,j,s}(t)\cos(j\theta)\right]\sin(\lambda_m x) + \sum_{m=1}^{M_2} v_{m,0}(t)\sin(\lambda_m x), \tag{18b}$$

$$w(x,\theta,t) = \sum_{m=1}^{M_1}\sum_{j=1}^{N}\left[w_{m,j,c}(t)\cos(j\theta) + w_{m,j,s}(t)\sin(j\theta)\right]\sin(\lambda_m x) + \sum_{m=1}^{M_2} w_{m,0}(t)\sin(\lambda_m x), \tag{18c}$$

where j is the number of circumferential waves, m the number of longitudinal half-waves, $\lambda_m = m\pi/L$, and t the time; $u_{m,j}(t)$, $v_{m,j}(t)$ and $w_{m,j}(t)$ are the generalized coordinates that are unknown functions of t; the additional subscript c or s indicates if the generalized coordinate is associated to a cosine or sine function in θ, except for v, for which the notation is reversed (no additional subscript is used for the axisymmetric terms). The integers N, M_1 and M_2 must be selected with care in order to obtain the required accuracy and acceptable dimension of the nonlinear problem.

Excitation in the neighbourhood of resonance of a mode with one longitudinal half-wave ($m = 1$) and n circumferential waves, denoted as mode (1, n), is considered. In particular, only modes with an odd m value of longitudinal half-waves can be considered for symmetry reasons in the expansions of v and w (if geometric imperfections with an even m value are not introduced); only even terms are necessary for u. Asymmetric modes having up to 12 longitudinal half-waves ($M_1 = M_2 = 12$) have been considered in the numerical calculations to achieve good accuracy. In fact, linear and nonlinear interaction among terms with different numbers of axial half-waves exists; these terms are not the linear modes of the shell with boundary conditions given by Eqs. (12). More terms are necessary for in-plane than for radial displacements.

The expansion used in the numerical calculation for excitation in the neighbourhood of resonance of mode (1, n) is

$$u(x,\theta,t) = \sum_{m=1}^{6}\left[u_{2m,n,c}(t)\cos(n\theta) + u_{2m,n,s}(t)\sin(n\theta)\right]\cos(\lambda_{2m}x) + \sum_{m=1}^{6} u_{2m,0}(t)\cos(\lambda_{2m}x) + \left[u_{2,2n,c}(t)\cos(2n\theta) + u_{2,2n,s}(t)\sin(2n\theta)\right]\cos(\lambda_2 x), \tag{19a}$$

$$v(x,\theta,t) = \sum_{m=1}^{6}[v_{2m-1,n,c}(t)\,\sin(n\theta) + v_{2m-1,n,s}(t)\,\cos(n\theta)]\,\sin(\lambda_{2m-1}x) + [v_{1,2n,c}(t)\,\sin(2n\theta) + v_{1,2n,s}(t)\,\cos(2n\theta)]\,\sin(\lambda_1 x) + [v_{3,2n,c}(t)\,\sin(2n\theta) + v_{3,2n,s}(t)\,\cos(2n\theta)]\,\sin(\lambda_3 x), \tag{19b}$$

$$w(x,\theta,t) = \sum_{m=1}^{6}[w_{2m-1,n,c}(t)\,\cos(n\theta) + w_{2m-1,n,s}(t)\,\sin(n\theta)]\,\sin(\lambda_{2m-1}x) + \sum_{m=1}^{6} w_{2m-1,0}(t)\,\sin(\lambda_{2m-1}x). \tag{19c}$$

This expansion has 54 generalized coordinates (dof) and guarantees good accuracy for the calculation performed in the present work, as numerically verified. The dimension of the nonlinear system is much smaller than 54 dof, but a different basis must be used to condense the system. However, this basis is very intuitive and allows calculations without losing the physical significance of each term. Torsional axisymmetric terms are not necessary.

Expansion (19) is an extension of the one developed for simply supported shells (Amabili, 2003c), for which convergence has been deeply investigated. In particular, more terms are necessary with respect to those used in Amabili (2003c) in order to have an accurate evaluation of the natural (linear) frequency, because the functions used are different from the mode shapes of the shell with constrained axial displacement ($u = 0$) at the shell ends. The inclusion of some extra terms, such as $u_{4,2n,c}(t)$ and $u_{4,2n,s}(t)$, has been checked numerically and does not give any significant change in the shell response.

2.5. External loads

For Model 1, the external harmonic excitation at point $(\bar{x},\bar{\theta})$ is assumed to be in the form of

$$f = \bar{f}\delta(\theta-\bar{\theta})\delta(x-\bar{x})\cos(\omega t), \tag{20}$$

where $\bar{f}$ is the amplitude of the force, and $\bar{\theta} = \bar{y}/R$ and $\bar{x}$ are the angular and axial coordinates of the point of application of the force. In this study, $\bar{y} = 0$ and $\bar{x} = L/2$.

For Model 2, the virtual work W done by the external forces is written as

$$W = \int_0^{2\pi}\int_0^{L}(q_x u + q_\theta v + q_r w)\,\mathrm{d}x R\,\mathrm{d}\theta, \tag{21}$$

where q_x, q_θ and q_r are the distributed forces per unit area acting in the axial, circumferential and radial directions, respectively. Initially, only a single harmonic radial force is considered; therefore $q_x = q_\theta = 0$. The external radial distributed load q_r applied to the shell, due to the radial concentrated force $\tilde{f}$, is given by

$$q_r = \tilde{f}\delta(R\theta - R\tilde{\theta})\delta(x-\tilde{x})\cos(\omega t), \tag{22}$$

where ω is the excitation frequency, t the time, δ the Dirac delta function, $\tilde{f}$ gives the radial force amplitude positive in the z direction, $\tilde{x}$ and $\tilde{\theta}$ give the axial and angular positions of the point of application of the force, respectively; in the numerical calculations, the point excitation is located at $\tilde{x} = L/2$, $\tilde{\theta} = 0$. Eq. (21) can be rewritten in the following form:

$$W = \tilde{f}\,\cos(\omega t)(w)_{x=L/2,\theta=0}. \tag{23}$$

The external force in Eqs. (20) and (23) can describe the excitation provided by an electrodynamical exciter (shaker), for instance.

2.6. Fluid–structure interaction

Let us consider the case when there is fluid–structure interaction. The shell is assumed to be completely filled with dense fluid. Furthermore, it is assumed, that the fluid is inviscid and isentropic. Nonlinearities in the dynamic pressure and in the boundary conditions at the fluid–structure interface are neglected, because fluid movements of the order of the shell thickness may be considered to be small; and hence a linear formulation is valid. Indeed, these nonlinear effects have been found to be negligible by Gonçalves and Batista (1988). In addition, pre-stress in the shell due to fluid weight (hydrostatic effect) is neglected. With these assumptions, the fluid–structure interaction can be described by potential flow theory.

We define the velocity potential by Φ. Neglecting compressibility effects, Φ must satisfy

$$\nabla^2\Phi = \frac{\partial^2\Phi}{\partial x^2} + \frac{\partial^2\Phi}{\partial r^2} + \frac{1}{r}\frac{\partial\Phi}{\partial r} + \frac{1}{r^2}\frac{\partial^2\Phi}{\partial\theta^2}, \tag{24}$$

i.e., the Laplace equation in cylindrical coordinates. Using Bernoulli's equation, the perturbation pressure p is easily found to be given by

$$p = \rho_F\left(\frac{\partial\Phi}{\partial t}\right). \tag{25}$$

In both models, the fluid is assumed to effectively be a deformable cylinder of infinite length, which lies within a periodically supported shell of infinite length. This assumption allows us to use the method of separation of variables in the solution of the velocity potential. This is possible only if we assume that the shell deformation w, along with the flow field, is defined for any $x \in (-\infty, \infty)$.

Specifically in Model 1, this requires that the modal expansion be equal to its antisymmetric expression between $x = L$ and $2L$, as follows:

$$\begin{aligned} w &= w(x, y, t) \qquad \text{for } 0 \leqslant x \leqslant L, \\ w &= -w(x - L, y, t) \quad \text{for } L \leqslant x \leqslant 2L\,. \end{aligned} \tag{26}$$

In essence, this periodicity of w allows us not to have to impose fluid boundary conditions at the ends of the finite $(0,L)$ domain of the shell. The periodicity for w, from 0 to $2L$, is important for the axisymmetric modes (modes with $n = 0$), so that a zero mean flow volume be obtained from 0 to $2L$.

The expression for w, in both models, satisfies the essential boundary conditions exactly for $0 \leqslant x \leqslant 2L$. It must satisfy the radial boundary conditions given by

$$\begin{aligned} &\text{at } r = 0 \text{ the flow is finite,} \\ &\text{at } r = R \Rightarrow \frac{\partial\Phi}{\partial r} = \left(\frac{\partial w}{\partial t}\right), \end{aligned} \tag{27}$$

where the second is the impermeability condition, applied at $r = R$. The expansion for w is substituted into the Laplace equation (24) and the solution for Φ is obtained with the separation of variables method. The velocity potential can be assumed to be of the form

$$\Phi(x, r, \theta, t) = \eta(r)\xi(x)g(\theta)\zeta(t). \tag{28}$$

Eq. (28) is substituted in Eq. (24), and the following three ordinary differential equations are obtained for x, r and θ:

$$\begin{aligned} &\eta''(r) + \frac{1}{r}\eta'(r) - \left(\frac{n^2}{r^2} - k_m^2\right)\eta(r) = 0, \\ &\xi''(x) + k_m^2\xi(x) = 0, \\ &g''(\theta) + n^2 g(\theta) = 0, \end{aligned} \tag{29}$$

where $(\,)'$ denotes a derivative with respect to r, x or θ, accordingly.

For Model 1, the solutions of Eqs. (29) are given by

$$\eta(r) = D_m \mathrm{I}_n(k_m r) + E_m \mathrm{K}_n(k_m r), \tag{30}$$

$$\xi(x) = A_m \sin(k_m x) + B_m \cos(k_m x), \tag{31}$$

$$g(\theta) = F \cos(n\theta), \tag{32}$$

where A_m, B_m, D_m, E_m and F are constants. The solutions of the above equations are found by expanding the radial displacement, w, as a Fourier series of an orthogonal set of functions, such as a sine series, thus transforming the beam functions of Eq. (14) into a series of sine functions of the same wavelength

$$w_{m,n} = \sum_{j=1}^{MM} b_{m,n,j} \sin\left(\frac{j\pi x}{L}\right) \cos(n\theta)\zeta(t), \tag{33}$$

where MM is an integer and

$$b_{m,n,j} = \frac{2}{L}\int_0^L \varphi_m(x)\,\sin\left(\frac{j\pi x}{L}\right)\mathrm{d}x, \tag{34}$$

where $\varphi_m(x)$ are the beam functions given by Eq. (14).

Using the impermeability boundary condition, Eq. (27), the solution for the velocity potential is found to be

$$\Phi = \sum_m \sum_n \frac{\eta_m(r)}{\eta'_m(r)|_{r=R}}\left[\frac{\partial w_{m,n}}{\partial t}\right]. \tag{35}$$

The final expression for the perturbation pressure term is found by substituting the velocity potential of Eq. (35) into the pressure Eq. (25).

For Model 2 the solution for the velocity potential, applying the condition of zero perturbation pressure at both ends of the shell ($(\Phi)_{x=0} = (\Phi)_{x=L} = 0$), is given by

$$\begin{aligned}\Phi = &\sum_{m=1}^{\infty}\sum_{n=0}^{\infty}[\alpha_{mn}(t)\cos(n\theta) + \beta_{mn}(t)\sin(n\theta)]\\ &\times[c_{mn}\mathrm{I}_n(\lambda_m r) + d_{mn}\mathrm{K}_n(\lambda_m r)]\sin(\lambda_m x),\end{aligned} \tag{36}$$

where $\mathrm{I}_n(r)$ and $\mathrm{K}_n(r)$ are the modified Bessel functions of the first and second kind, respectively, of order n, and $\lambda_m = m\pi/L$. By using the assumed mode expansion of w, given by Eq. (19c), and applying the impermeability condition (27), the solution of the boundary value problem for internal fluid only is

$$\Phi = -\sum_{m=1}^{M}\sum_{n=0}^{N}[\dot{w}_{m,n,c}(t)\,\cos(n\theta) + \dot{w}_{m,n,s}(t)\sin(n\theta)]\,\frac{\mathrm{I}_n(\lambda_m r)}{\lambda_m \mathrm{I}'_n(\lambda_m R)}\,\sin(\lambda_m x), \tag{37}$$

where $\mathrm{I}'_n(r)$ is the derivative of $\mathrm{I}_n(r)$ with respect to r, and M the largest between M_1 and M_2, introduced in Eq. (18). Axisymmetric generalized coordinates are included with the others involving subscript c, for brevity. Therefore, the perturbation pressure p exerted by the contained fluid on the shell is given by

$$p = \rho_F(\dot{\Phi})_{r=R} = -\rho_F\sum_{m=1}^{M}\sum_{n=0}^{N}[\ddot{w}_{m,n,c}(t)\,\cos(n\theta) + \ddot{w}_{m,n,s}(t)\,\sin(n\theta)]\,\frac{\mathrm{I}_n(\lambda_m R)}{\lambda_m \mathrm{I}'_n(\lambda_m R)}\,\sin(\lambda_m x), \tag{38}$$

where ρ_F is the mass density of the internal fluid. Eq. (38) shows that the fluid has an inertial effect on radial motion of the shell. In particular, this inertial effect is different for the asymmetric and the axisymmetric terms of the mode expansion. Hence, the fluid is expected to change the nonlinear behaviour of the fluid-filled shell. Usually the inertial effect of the fluid is larger for axisymmetric modes, thus enhancing the nonlinear behaviour of the shell.

The difference in sign between (35) and (37) is because of the difference in the positive direction for w.

2.7. Method of solution

2.7.1. Solution method for Model 1

For Model 1, the expression for w, given in Eq. (17), is substituted into Eq. (2) to obtain a solution for the Airy stress function F. The solution of F is composed of a particular solution F_p and a homogeneous solution F_h. For the 7 dof model, all 280 terms of the particular solution are satisfied exactly, by ensuring the correspondence (one by one) between the right-hand side terms of Eq. (2) with appropriate solution terms on the left-hand side of the same expression. This is an arduous task, fraught with numerical difficulties, because of the hyperbolic functions involved in the modal expansion. The homogeneous solution for the Airy stress function is assumed to be of the form

$$\begin{aligned}F_h = &\left\{\frac{1}{2}\bar{N}_x y^2 - \frac{1}{2\pi RL}\int_0^{2\pi R}\int_0^L\left[\frac{\partial^2 F_p}{\partial y^2}\right]\mathrm{d}y\,\mathrm{d}x\right\} + \left\{\frac{1}{2}\bar{N}_y x^2 - \frac{1}{2\pi RL}\int_0^{2\pi R}\int_0^L\left[\frac{\partial^2 F_p}{\partial x^2}\right]\mathrm{d}y\,\mathrm{d}x\right\}\\ &- \left\{\bar{N}_{xy}xy - \frac{1}{2\pi RL}\int_0^{2\pi R}\int_0^L\left[\frac{\partial^2 F_p}{\partial x\partial y}\right]\mathrm{d}y\,\mathrm{d}x\right\}.\end{aligned} \tag{39}$$

The homogeneous solution includes the influence of the average particular solution to the averaged forces per unit length. These latter are calculated using the expressions in Eq. (4) and averaging them over the circumference and length of the shell (denoted by the overbars in Eq. (39)). The final expression of Eq. (1), including the solutions for the fluid–structure interaction and the point-force external harmonic function, is discretized to seven ordinary differential

equations using the comparison functions $\phi_i(x, y)$,

$$\phi_i(x,y) = \begin{cases} \phi_1 = \varphi_1 \cos(ny/R), \\ \phi_2 = \varphi_1 \sin(ny/R), \\ \phi_3 = \varphi_2 \cos(ny/R), \\ \phi_4 = \varphi_2 \sin(ny/R), \\ \phi_5 = \varphi_1, \\ \phi_6 = \varphi_3, \\ \phi_7 = \varphi_5, \end{cases} \tag{40}$$

by means of the Galerkin technique. The φ_i in the expression above are the clamped–clamped beam eigenfunctions.

2.7.2. Solution method for Model 2

In the case of Model 2, the Hamiltonian (variational) approach is used leading to a Lagrangian derivation of the discretized equations of motion. The potential and kinetic energies related to the external loading and added mass are inserted to the stress–strain potential and kinetic relationships as follows.

Using Green's theorem, the kinetic energy associated with the fluid is given by

$$T_F = \frac{1}{2}\rho_F \int_0^{2\pi} \int_0^L (\Phi)_{r=R} \dot{w}\, \mathrm{d}x R\, \mathrm{d}\theta. \tag{41}$$

The nonconservative damping forces are assumed to be of the viscous type and could be taken into account by using Rayleigh's dissipation function; however, in what follows, for comparison with experiment, we consider c to have a different value for each term of the mode expansion. Simple calculations give

$$F = \frac{1}{2}(L/2)R \sum_{n=0}^{N} \sum_{m=1}^{M} \psi_n [c_{m,n,c}(\dot{u}_{m,n,c}^2 + \dot{v}_{m,n,c}^2 + \dot{w}_{m,n,c}^2) + c_{m,n,s}(\dot{u}_{m,n,s}^2 + \dot{v}_{m,n,s}^2 + \dot{w}_{m,n,s}^2)], \tag{42}$$

where

$$\psi_n = \begin{cases} 2\pi & \text{if } n = 0, \\ \pi & \text{if } n > 0. \end{cases} \tag{43}$$

The damping coefficient $c_{m,n,c \text{ or } s}$ is related to a modal damping ratio, that can be evaluated from experiments, by $\varsigma_{m,n,c \text{ or } s} = c_{m,n,c \text{ or } s}/(2\mu_{m,n}\omega_{m,n})$, where $\omega_{m,n}$ is the natural circular frequency of mode (m, n) and $\mu_{m,n}$ is the modal mass of this mode, given by $\mu_{m,n} = \psi_n(\rho_S + \rho_V)h(L/2)R$, and the virtual mass due to contained fluid is

$$\rho_V = \frac{\rho_F}{\lambda_m h} \frac{\mathrm{I}_n(\lambda_m R)}{\mathrm{I}'_n(\lambda_m R)}. \tag{44}$$

The total kinetic energy of the system is

$$T = T_S + T_F. \tag{45}$$

The potential energy of the system is given by the sum of the elastic strain energy of the shell and the energy stored by the two distributed rotational springs at the shell edges

$$U = U_S + U_R. \tag{46}$$

The virtual work done by the concentrated radial force $\tilde{f}$, expressed by Eq. (23), is specialized for the expression of w given in Eq. (18c)

$$W = \tilde{f}\cos(\omega t)(w)_{x=L/2,\ \theta=0} = \tilde{f}\cos(\omega t)\left[\sum_{m=1}^{M_1}\sum_{j=1}^{N} w_{m,j,c}(t) + \sum_{m=1}^{M_2} w_{m,0}(t)\right]. \tag{47}$$

The following notation is introduced for brevity:

$$\mathbf{q} = \{u_{m,n,c}, u_{m,n,s}, v_{m,n,c}, v_{m,n,s}, w_{m,n,c}, w_{m,n,s}\}^{\mathrm{T}}, m = 1, \ldots, M \text{ and } n = 0, \ldots, N. \tag{48}$$

The generic element of the time-dependent vector $\mathbf{q}$ is referred to as q_j; the dimension of $\mathbf{q}$ is equal to the number of dof used in the modal expansion.

The generalized forces Q_j are obtained by differentiation of Rayleigh's dissipation function and of the virtual work done by external forces

$$Q_j = -\frac{\partial F}{\partial \dot{q}_j} + \frac{\partial W}{\partial q_j} = -c_j \dot{q}_j + \begin{cases} 0 & \text{if } q_j = u_{m,n,c/s},\ v_{m,n,c/s} \text{ or } w_{m,n,s}, \\ \tilde{f}\cos(\omega t) & \text{if } q_j = w_{m,n,c}, \end{cases} \tag{49}$$

where the subscript c/s indicates c or s.

The Lagrange equations of motion for the fluid-filled shell are

$$\frac{\mathrm{d}}{\mathrm{d}t}\left(\frac{\partial T}{\partial \dot{q}_j}\right) - \frac{\partial T}{\partial q_j} + \frac{\partial U}{\partial q_j} = Q_j, \quad j = 1, \ldots, \mathrm{dof}, \tag{50}$$

where $\partial T/\partial q_j = 0$. These second-order equations have very long expressions, containing quadratic and cubic nonlinear terms. In particular,

$$\frac{\mathrm{d}}{\mathrm{d}t}\left(\frac{\partial T}{\partial \dot{q}_j}\right) = \begin{cases} \rho_S h(L/2)\psi_n R\ddot{q}_j & \text{if } q_j = u_{m,n,c/s} \text{ or } v_{m,n,c/s}, \\ (\rho_S + \rho_V)h(L/2)\psi_n R\ddot{q}_j & \text{if } q_j = w_{m,n,c/s}, \end{cases} \tag{51}$$

which shows that no inertial coupling exists in this case.

The very complicated term giving quadratic and cubic nonlinearities can be written in the form

$$\frac{\partial U}{\partial q_j} = \sum_{k=1}^{\mathrm{dof}} q_k f_k + \sum_{i,k=1}^{\mathrm{dof}} q_i q_k f_{i,k} + \sum_{i,k,l=1}^{\mathrm{dof}} q_i q_k q_l f_{i,k,l}, \tag{52}$$

where coefficients f have long expressions which can also include geometric imperfections.

3. Numerical results

The equations of motion have been obtained using the *Mathematica* version 4 computer software (Wolfram, 1999) in order to perform analytical surface integrals of trigonometric functions. For both models, the discretized second-order differential equations are transformed into two first-order equations. A nondimensionalization of variables is also performed for computational convenience: the frequencies are divided by the natural frequency $\omega_{m,n}$ of the mode (m, n) investigated, and the vibration amplitudes are divided by the shell thickness h. The resulting first-order ordinary differential equations are studied by using the software AUTO 97 (Doedel et al., 1998) for continuation and bifurcation analysis of nonlinear ordinary differential equations. The software AUTO 97 is capable of continuation of the solution, bifurcation analysis and branch switching by using arclength continuation and collocation methods. In particular, the shell response under harmonic excitation has been studied via an analysis in two steps: (i) with the excitation frequency fixed far enough from resonance, the magnitude of the excitation has been used as bifurcation parameter; the solution was started at zero force, where the solution is the trivial undisturbed configuration of the shell, and was continued up to the desired maximum force magnitude; (ii) when this desired magnitude of excitation was reached, the solution was then continued by using the excitation frequency as bifurcation parameter.

Calculations have been performed for a shell having the following dimensions and material properties: $L = 520\,\mathrm{mm}$, $R = 149.4\,\mathrm{mm}$, $h = 0.519\,\mathrm{mm}$, $E = 1.98 \times 10^{11}\,\mathrm{Pa}$, $\rho_S = 7800\,\mathrm{kg/m^3}$ and $v = 0.3$. This shell has a fundamental mode with six circumferential waves and one longitudinal half-wave ($n = 6$, $m = 1$) for clamped boundary conditions given by Eqs. (11) and (12). Calculations with the shell either empty or completely water-filled ($\rho_F = 1000\,\mathrm{kg/m^3}$) are presented in the following subsection.

3.1. Numerical results for empty and water filled shells

Table 1 lists the theoretical results obtained by the two models presented in this paper, along with the results of Rayleigh–Ritz code DIVA, for the frequency of the fundamental mode ($n = 6$, $m = 1$) for empty and water-filled shell.

Table 1
Fundamental natural frequency ($n = 6$, $m = 1$) of empty and water-filled clamped shells calculated using Rayleigh–Ritz code (DIVA) and Models 1 and 2

Model	Empty shell frequency (Hz)	Water-filled frequency (Hz)
DIVA	315.1	119.8
Model 1	340.3	127.9
Model 2	326.7	124.3

The software DIVA was used along with Flügge's shell theory and 60 longitudinal modes to produce the frequency of the empty shell as listed in Table 1. Model 1 used a 7 dof expansion derived from Eq. (13). Model 2 used the expansion given in Eqs. (19a–c) with a spring constant $k = 10^{10}$ N for boundary condition Eq. (12d) embedded in the boundary conditions to approximate the clamped ends.

The fundamental natural frequency predicted by Model 2 (Table 1), in the case of the empty shell, is in good agreement with that obtained by DIVA software (only 3.6% higher). Model 1 predicts a higher frequency (8% higher than DIVA) in the case of the empty shell. In the case of the water-filled shell, the differences between DIVA and Models 1 and 2 are smaller: 6.7% and 3.6%, respectively.

The frequency–amplitude response of the empty shell to a harmonic excitation of $\tilde{f} = \bar{f} = 3$ N in the neighbourhood of the fundamental mode ($n = 6$, $m = 1$), for both models is shown in Fig. 2; the results have been calculated assuming a modal damping of $\zeta_{1,n} = 0.001$. In Fig. 2 both models exhibit a hysteresis predicting a softening type of nonlinear response for the shell vibrations. There is a good qualitative and quantitative agreement between the theoretical results of the two models.

In the case of the water filled shell the frequency–amplitude responses with a forcing function of $\tilde{f} = \bar{f} = 3$ N with a modal damping of $\zeta_{1,n} = 0.0017$ for both models are shown in Fig. 3. Both models predict an unstable solution when the excitation frequency is in the range of $0.993 < \omega/\omega_{1,n} < 1.001$. In this frequency range there is a two-period quasiperiodic response with amplitude modulations, as shown in Amabili (2003a–c). The agreement between the two models is better in the case of the water-filled shell.

In both cases, for the empty and the water filled shell, the coexistence of modes having the same shape but different angular orientations, the first one described by $\cos(n\theta)$ (driven mode) and the other by $\sin(n\theta)$ (companion mode), in the periodic response leads to the appearance of travelling-wave vibration around the shell in the angular direction. This phenomenon is related to the axial-symmetry of the system and is a fundamental difference *vis-à-vis* linear vibrations. The presence of the companion mode in the shell response also leads to occurrence of more complex phase-relationships among the generalized coordinates (Amabili, 2003b). Away from resonance, the companion mode solution disappears and the generalized coordinates are nearly in phase or in anti-phase.

3.2. Comparison of theoretical and experimental results

Both models are compared to the experimental results obtained for a clamped polyester shell tested by Chiba (1993) having the following dimensions and material properties: $L = 480$ mm, $R = 240$ mm, $h = 0.254$ mm, $E = 4.65 \times 10^9$ Pa, $\rho_S = 1400\,\text{kg/m}^3$ and $\nu = 0.38$. Because the circular cylindrical shell had a longitudinal lap-joint seam, the axial-symmetry of the shell was broken and the measured response of the vibration mode ($n = 15$, $m = 1$) did not display a travelling wave. For this reason, the companion mode was eliminated from the expansion of the shell displacements in the theoretical models. The spring constant in Model 2 was set to $k = 10^8$ N, which is large enough to simulate clamped ends.

The natural frequency of the fundamental mode ($n = 15$, $m = 1$) was found to be 95.7 Hz, in both theoretical models. The numerical responses obtained by the two models, evaluated for a force level $\tilde{f} = \bar{f} = 0.02$ N and modal damping $\zeta_{1,n} = 0.0015$, are plotted in Fig. 4 and are compared to Chiba's backbone curve (giving the free-vibration resonance, corresponding to the maximum of the response versus the vibration frequency). Fig. 4 shows the same trend of a softening type nonlinearity computed by using the two models and Chiba's (1993) experimental results, but clearly there are some quantitative differences between the experimental data and the theoretical results.

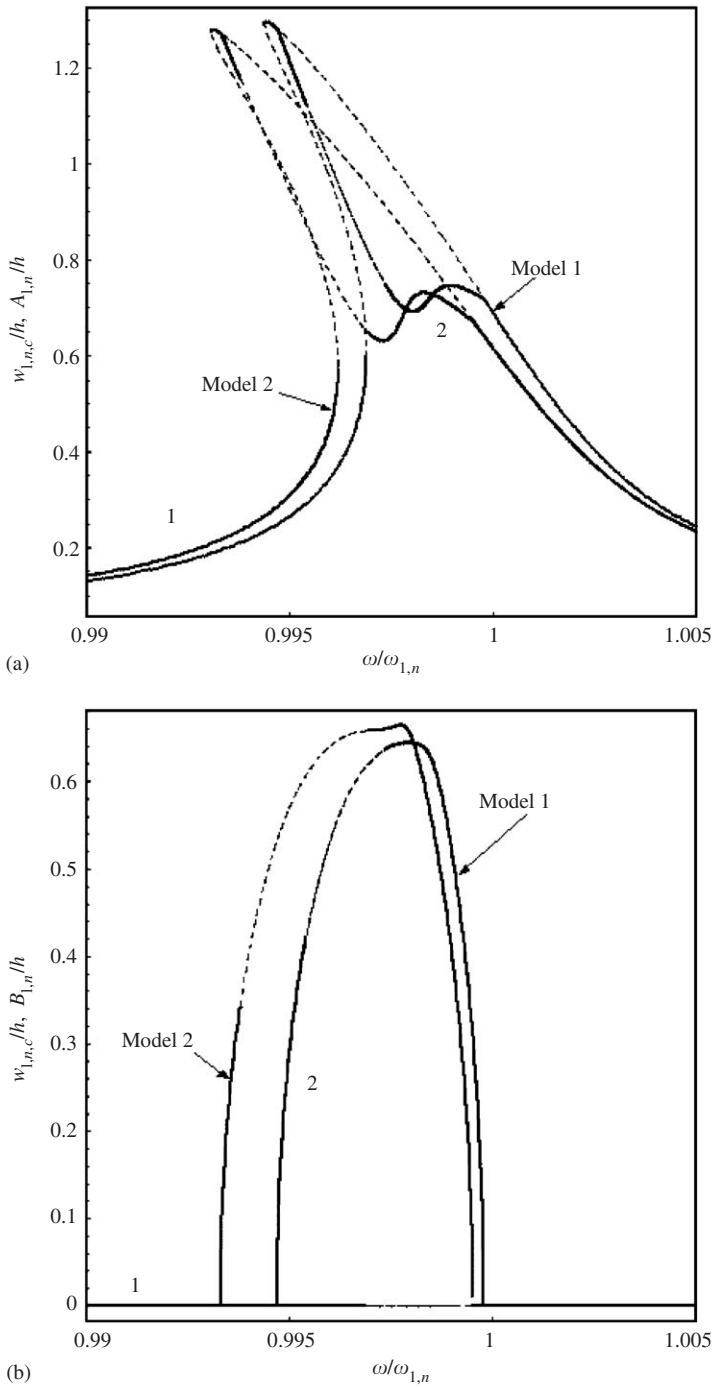

Fig. 2. The amplitude–frequency response of the fundamental mode, for an empty clamped shell, using Donnell's theory with $\zeta_{1,n} = 0.001$ and $\tilde{f} = \bar{f} = 3$ N: (1) branch 1; (2) branch 2; ——, stable response; - - - - -, unstable response. (a) Driven mode amplitude; and (b) companion mode amplitude.

4. Conclusions

Two theoretical models for clamped shells in contact with fluid have been developed to study the nonlinear vibrations of thin circular cylindrical shells. In Model 1, the classical Donnell nonlinear shallow-shell theory was used to describe

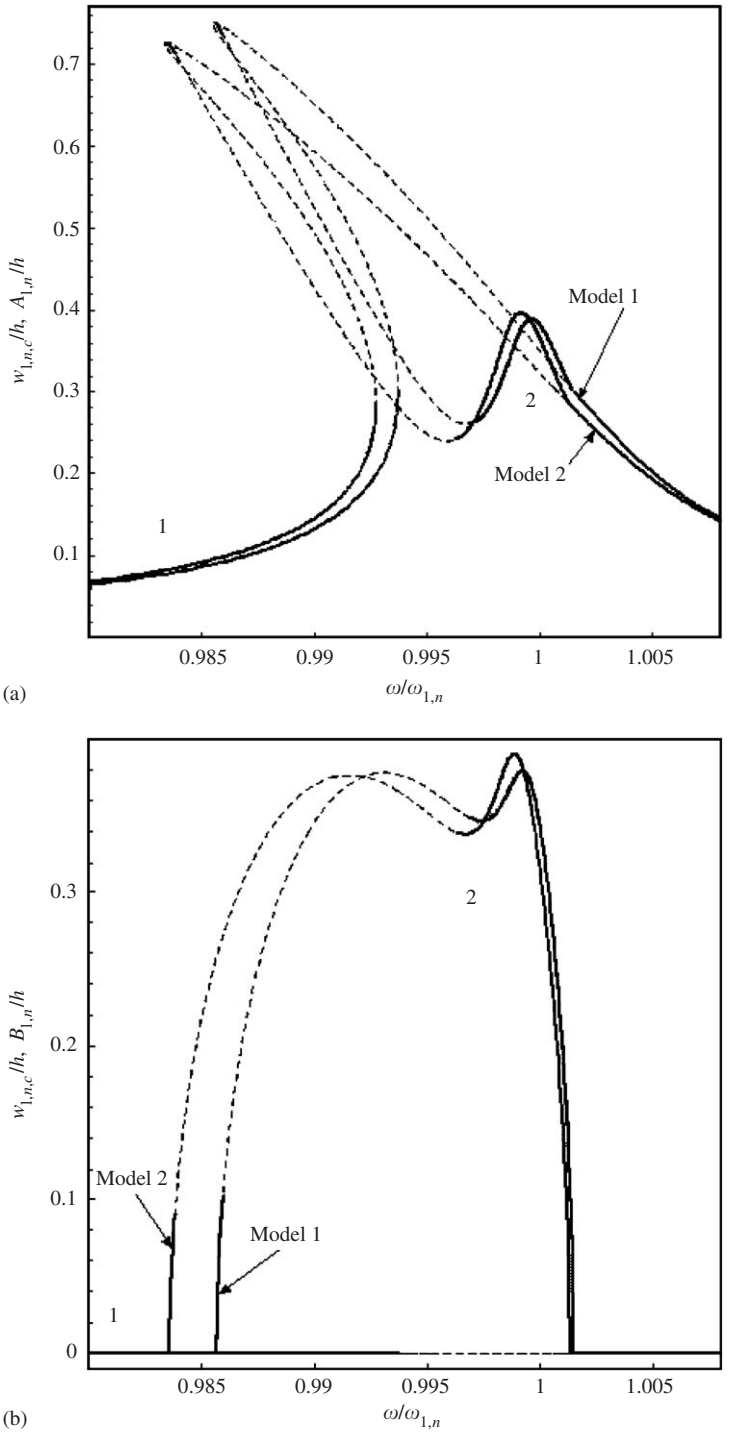

Fig. 3. The amplitude–frequency response of the fundamental mode, for a water filled clamped shell, using Donnell's theory with $\zeta_{1,n} = 0.0017$ and $\tilde{f} = \bar{f} = 3$ N: (1) branch 1; (2) branch 2; ——, stable response; - - - - -, unstable response. (a) Driven mode amplitude; and (b) companion mode amplitude.

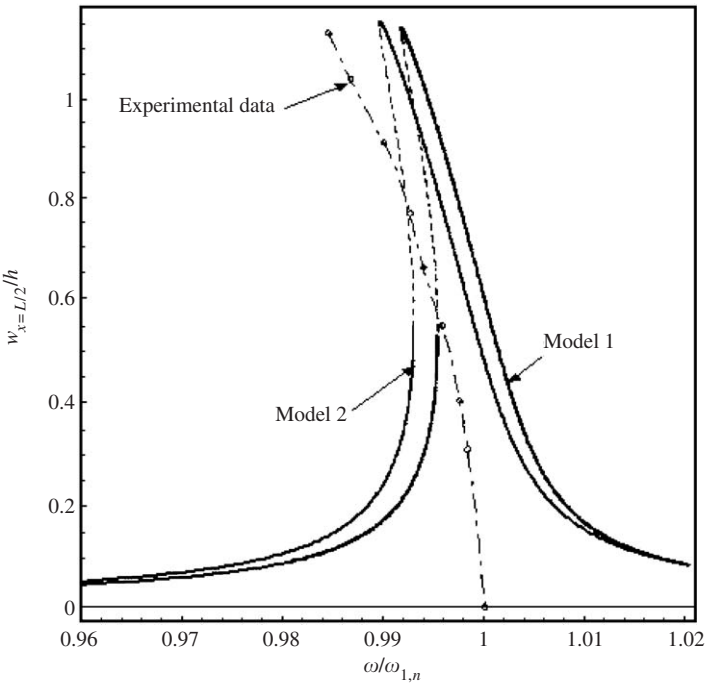

Fig. 4. The experimental (Chiba, 1993) and theoretical (Models 1, 2) amplitude–frequency response for the fundamental mode ($n = 15$, $m = 1$) of an empty shell using Donnell's theory and $\zeta_{1,n} = 0.0015, \tilde{f} = \bar{f} = 0.02$ N, with branch 1 only shown; shell displacement at excitation point $x = L/2$. ——, Theoretical stable response; ------, theoretical unstable response; ---○--, experimental backbone curve from Chiba.

the large amplitude vibrations of the shell. In Model 2, a flexible, energy approach has been used to construct a model applicable for very thin shells, which is suitable for simulating different boundary conditions via elastic constraints. In both models the shell deformation expansion includes the driven and companion modes, along with a sufficient number of axisymmetric terms to ensure the correct type of nonlinear response.

The nonlinearity is enhanced for a completely water-filled shell as compared to the same empty shell. Numerical results are compared to those available in the literature for both models. The difference in the results between Models 1 and 2 can be improved if more terms (asymmetric and axisymmetric) are included in the shell deformation expansions, especially in the case of Model 1.

Both models are based on Ritz-type methods and employ global basis functions. In this regard, it would have been interesting to compare the results with those obtained by finite element methods—not only the results themselves, but also computational times. This, however, is at present impracticable. In this regard, the two models used in this paper offer a great advantage over finite element codes for predicting the shell response close to resonance. The finite element codes require extensive calculations over a wide frequency spectrum close to resonance, using different time-marching integration techniques in order to obatin results. Therefore, these codes are time-consuming and usually require state-of-the-art hardware to deal with the memory-intensive calculations in the computer. However, the most difficult problem that these codes pose is the guess that must be made of the initial conditions for the shell surface in order to follow the solution in the bifurcation diagram. Any solution jumps due to transition of the solution from stable to unstable (and vice versa), or due to the appearance of additional stable and unstable solutions along with discontinuities that might exist in the shell response solution, are extremely difficult, if not impossible, to be dealt with in the existing finite element codes because of the initial condition limitations that such software impose. Additional problems with accuracy, convergence and prediction of the correct trend of shell nonlinearity make the use of finite element codes less desirable as compared to the solutions given by the two models in this paper.

Acknowledgments

The authors would like to thank NSERC of Canada and FCAR of Québec for their financial support of this research. This work was also partially supported by a FIRB and COFIN grants of the Italian Ministry for University and Research (MURST).

References

Amabili, M., 2003a. Nonlinear vibrations of circular cylindrical shells with different boundary conditions. AIAA Journal 41, 1119–1130.

Amabili, M., 2003b. Theory and experiments for large-amplitude vibrations of empty and fluid-filled circular cylindrical shells with imperfections. Journal of Sound and Vibration 262, 921–975.

Amabili, M., 2003c. Comparison of different shell theories for large-amplitude vibrations of empty and fluid-filled circular cylindrical shells with and without imperfections: Lagrangian approach. Journal of Sound and Vibration 264, 1091–1125.

Amabili, M., Garziera, R., 2000. Vibrations of circular cylindrical shells with nonuniform constraints, elastic bed and added mass; Part I: empty and fluid-filled shells. Journal of Fluids and Structures 14, 669–690.

Amabili, M., Païdoussis, M.P., 2003. Review of studies on geometrically nonlinear vibrations and dynamics of circular cylindrical shells and panels, with and without fluid–structure interaction. Applied Mechanics Reviews 56, 105–125.

Amabili, M., Pellicano, F., Païdoussis, M.P., 1999. Non-linear dynamics and stability of circular cylindrical shells containing flowing fluid. Part I: Stability. Journal of Sound and Vibration 225, 655–699.

Amabili, M., Pellicano, F., Païdoussis, M.P., 2000. Non-linear dynamics and stability of circular cylindrical shells containing flowing fluid. Part III: truncation effect without flow and experiments. Journal of Sound and Vibration 237, 617–640.

Chia, C.Y., 1987a. Non-linear free vibration and postbuckling of symmetrically laminated orthotropic imperfect shallow cylindrical panels with two adjacent edges simply supported and the other edges clamped. International Journal of Solids and Structures 23, 1123–1132.

Chia, C.Y., 1987b. Nonlinear vibration and postbuckling of unsymmetrically laminated imperfect shallow cylindrical panels with mixed boundary conditions resting on elastic foundation. International Journal of Solids and Structures 25, 427–441.

Chiba, M., 1993. Experimental studies on a nonlinear hydroelastic vibration of a clamped cylindrical tank partially filled with liquid. ASME Journal of Pressure Vessel Technology 115, 381–388.

Doedel, E.J., Champneys, A.R., Fairgrieve, T.F., Kuznetsov, Y.A., Sandstede, B., Wang, X., 1998. AUTO 97: Continuation and Bifurcation Software for Ordinary Differential Equations (with HomCont). Concordia University, Montreal, Canada.

Donnell, L.H., 1976. Beams, Plates, and Shells. McGraw-Hill, Inc., New York.

Dowell, E.H., Ventres, C.S., 1968. Modal equations for the nonlinear flexural vibrations of a cylindrical shell. International Journal of Solids and Structures 4, 975–991.

Fu, Y.M., Chia, C.Y., 1993. Non-linear vibration and postbuckling of generally laminated circular cylindrical thick shells with non-uniform boundary conditions. International Journal of Non-Linear Mechanics 28, 313–327.

Gonçalves, P.B., Batista, R.C., 1988. Non-linear vibration analysis of fluid-filled cylindrical shells. Journal of Sound and Vibration 127, 133–143.

Gunawan, L., 1998. Experimental study of nonlinear vibrations of thin-walled cylindrical shells. Ph.D. Thesis, Faculty of Aerospace Engineering, Technische Universiteit Delft, The Netherlands.

Iu, V.P., Chia, C.Y., 1988. Non-linear vibration and postbuckling of unsymmetric cross-ply circular cylindrical shells. International Journal of Solid Structures 24, 195–210.

Kobayashi, Y., Leissa, A.W., 1995. Large-amplitude free vibration of thick shallow shells supported by shear diaphragms. International Journal of Non-Linear Mechanics 30, 57–66.

Leissa, A.W., 1973. Vibration of Shells, NASA SP-288. Government Printing Office, Washington, DC now available from The Acoustical Society of America (1993).

Matsuzaki, Y., Kobayashi, S., 1969. A theoretical and experimental study of the nonlinear flexural vibration of thin circular shells with clamped ends. Transactions of the Japan Society for Aeronautical and Space Sciences 12, 55–62.

Païdoussis, M.P., 2003. Fluid–Structure Interactions. Slender Structures and Axial Flow, vol. 2. Elsevier Academic Press, London.

Wolfram, S., 1999. The Mathematica Book, fourth ed. Cambridge University Press, Cambridge.

Yamaki, N., 1984. Elastic Stability of Circular Cylindrical Shells. North-Holland, Amsterdam.

Yuan, J., Dickinson, S.M., 1992. On the use of artificial springs in the study of the free vibrations of systems comprised of straight and curved beams. Journal of Sound and Vibration 152, 203–216.